PCCP

Exploring molecular motions in collinear HeH_2^+ and its isotopic variants using periodic orbits

Pankaj Bhatia,[a]* Biswajit Maiti,[a] Narayanasami Sathyamurthy,[a]† Stamatis Stamatiadis,[b]‡ and Stavras C. Farantos[b]§

[a] *Department of Chemistry, Indian Institute of Technology, Kanpur 208 016, India*
[b] *Institute of Electronic Structure and Laser, Foundation for Research and Technology Hellas, Iraklion, Crete, 711 10, Greece*

Received 28th October 1998, Accepted 8th January 1999

Principal families of periodic orbits (POs) are identified and their (in)stabilities examined for collinear HeH_2^+ and its isotopic variants, $HeHD^+$ and $HeDH^+$, on an *ab initio* potential energy surface. Continuation/bifurcation diagrams of these periodic orbits over a range of energies reveal a number of bifurcations and the period doubling route to classical chaos. The existence of a number of POs at any given energy suggests that there could be constructive and destructive interference between their contributions to the eigenfunction at that energy resulting in quantum mechanical resonances for these systems.

1 Introduction

Resonances in collinear (He, H_2^+) collisions have been the subject of investigation for the last several years. Quantum mechanical calculations of the reaction

$$He + H_2^+ \rightarrow HeH^+ + H \quad (1)$$

in collinear geometry by Kouri and Baer[1] and Adams,[2] on a diatomics-in-molecules[3] potential energy surface (PES), revealed a large number of oscillations in plots of vibrational (v) state-selected reaction probability (P_v^R) as a function of total energy (E = relative translational energy of reactants + vibrational energy of the reactant molecule). Chapman and Hayes[4] found that inelastic transition probabilities below the reaction threshold also varied dramatically with E and that most of the oscillations were owing to Feshbach (compound state or closed channel) resonances and that some were owing to open channel resonances. Quantum calculations[5] on a more accurate *ab initio* potential energy surface,[6] fitted to an analytic function[7] (hereinafter referred to as MTJS PES), also revealed a large number of oscillations in the $P_v^R(E)$ plots for $v = 0$–4 and many of the resonances were interpreted[8] in terms of bound states supported by vibrational adiabatic potentials in hyperspherical coordinates.[9] Further calculations[10,11] revealed a large number of oscillations; some of them have been identified as threshold resonances but a number of them still remain unaccounted for. A time-dependent quantum mechanical (TDQM) investigation[12] of a Gaussian wave packet located initially in the interaction region and evolving on the MTJS PES yielded the time correlation function $C(t)$, Fourier transform of which resulted in the power spectrum. The number of peaks and their positions in the spectrum corroborated the existence of a large number of quantum mechanical resonances in the system. An analysis of the spacing between levels in the power spectrum pointed to the existence of quantum chaos[13] in this system, which also exhibits classical chaos.[14]

When one of the two H atoms in HeH_2^+ is replaced by D, we get some very interesting results:[15] $P_v^R(E)$ has a staircase-like structure for the reaction

$$He + HD^+ \rightarrow HeH^+ + D \quad (2)$$

but a highly oscillatory structure for

$$He + DH^+ \rightarrow HeD^+ + H \quad (3)$$

Further investigations[16] reveal a more irregular behavior (classical as well as quantal) for reactive (He, DH^+) dynamics than for (He, HD^+). It also becomes clear that the kinematic factors play an important role in the dynamics of the system.[17] Similar findings have been reported for the HCP/DCP molecules.[18–20]

Details of the TDQM methodology and the eigenvalue spectra obtained for collinear HeH_2^+, $HeHD^+$ and $HeDH^+$ have been reported earlier.[12,15] Still, for the sake of clarity and completeness, we show in Fig. 1 the spectra obtained at three different resolutions, for collinear HeH_2^+ by Fourier transforming $C(t)$ computed for a Gaussian wave packet centered initially in the interaction region and time evolved in scaled and skewed coordinates[21] for three different lengths of time. The low resolution spectrum resulting from $C(t)$ over 2048 timesteps (1 timestep = 0.161 625 fs), and shown as the uppermost curve, reveals certain regularity. But the one in the middle, obtained at a higher resolution by the use of $C(t)$ over double the number of timesteps, reveals additional peaks. The spectrum in the lowest curve, obtained from $C(t)$ over 32 768 timesteps, exhibits an even more complicated structure. The spectrum consists of two bound states for $E < 0$. For $E > 0$, the spectrum starts off regular but becomes highly irregular with increasing energy.

Plots of probability density contours for the eigenfunctions ($|\Psi|^2$) corresponding to different eigenvalues of the Hamiltonian, shown in Fig. 2 at low energies, account for the regularity in the spectrum in that energy range. They can be easily assigned quantum numbers (0,0), (1,0), (2,0) and (2,1) corre-

* Present address: Department of Chemistry, Massachusetts Institute of Technology, 77 Massachusetts Avenue, Cambridge, MA 02139, USA.
† Honorary Professor, S. N. Bose National Centre for Basic Sciences, Calcutta India.
‡ Also at the Department of Physics, University of Crete, Iraklion 7110, Crete, Greece.
§ Also at the Department of Chemistry, University of Crete, Iraklion 7110, Crete, Greece.

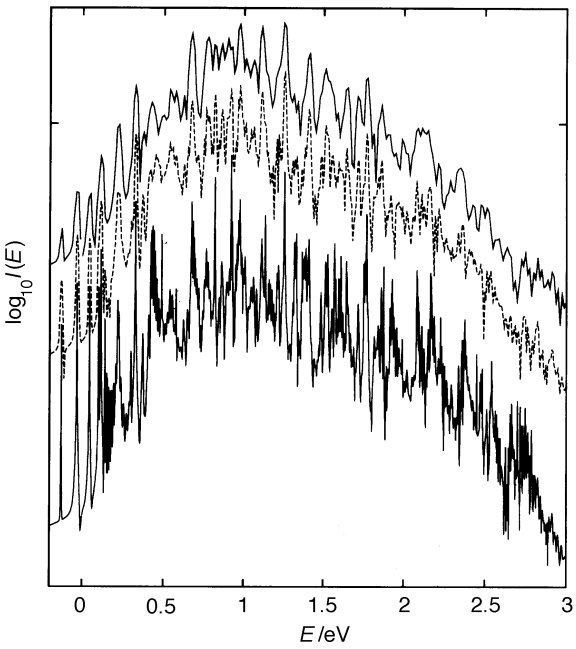

Fig. 1 Eigenvalue spectrum for collinear HeH_2^+ as obtained from time evolving a Gaussian wave packet centered in the interaction region in (q_1, q_2) coordinates at different resolutions: the uppermost curve, from Fourier transforming $C(t)$ over 2048 timesteps (1 timestep = 0.161 625 fs), the middle one from $C(t)$ over 4096 timesteps and the lowest curve from $C(t)$ over 32 768 timesteps.

sponding to (q_1, q_2) coordinates; the associated eigenvalues are listed in Table 1. Similar plots for some of the peaks at higher energies also reveal a certain regularity: they correspond to hyperspherical modes and can also be assigned a set of quantum numbers (n_r, n_θ) along radial and angular directions, as shown in Fig. 3. A list of eigenvalues corresponding to the clearly identified hyperspherical modes and their assignments is given in Table 2. There exist a set of periodic orbits (POs) that are superimposable on these $|\Psi|^2$ plots as illustrated in those figures. But contour plots of $|\Psi|^2$ corresponding to a large number of other peaks in the spectrum are quite complex (for example, see Fig. 4) and they can not be assigned readily. Efforts to identify particular POs that correspond to these eigenfunctions have not been successful (see below).

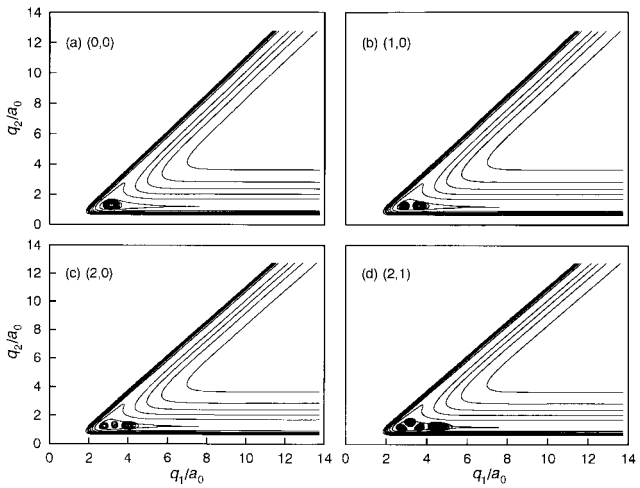

Fig. 2 Plots of $|\Psi|^2$ for eigenfunctions of collinear HeH_2^+ near the zero of energy, superimposed on the potential energy contours for the system. The quantum numbers in different panels refer to local modes and can be discerned readily from the nodal structures of $|\Psi|^2$. The corresponding eigenvalues are listed in Table 1.

Table 1 Eigenvalues and the local mode assignments in (q_1, q_2) coordinates for collinear HeH_2^+

E/eV	(n_1, n_2)
−0.128	(0, 0)
−0.032	(1, 0)
0.044	(2, 0)
0.099	(2, 1)

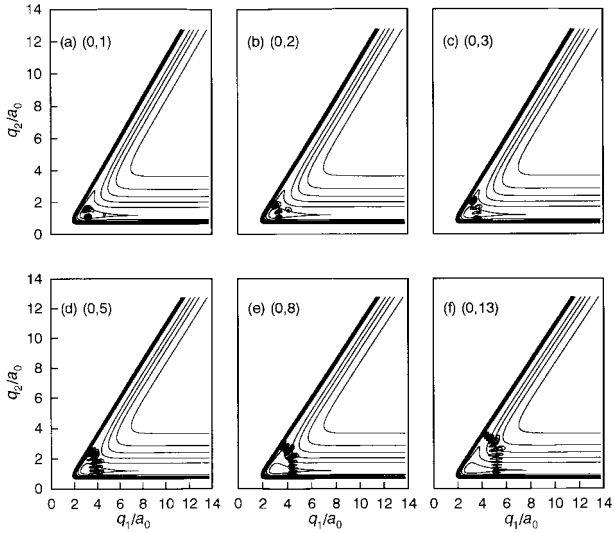

Fig. 3 Plots of $|\Psi|^2$ for hyperspherical modes of collinear HeH_2^+ superimposed on the potential energy contours for the system. The corresponding quantum numbers are included in different panels and eigenvalues are listed in Table 2. Superimposed in panels (b) and (f) are the periodic orbits of hyperspherical variety, for illustration.

Table 2 Eigenvalues corresponding to hyperspherical modes with quantum numbers (n_r, n_θ) in radial and angular directions, respectively, for collinear HeH_2^+

E/eV	(n_r, n_θ)
0.114	(0, 1)
0.325	(0, 2)
0.488	(0, 3)
0.817	(0, 5)
1.253	(0, 8)
1.875	(0, 13)
1.990	(0, 14)
2.189	(0, 16)

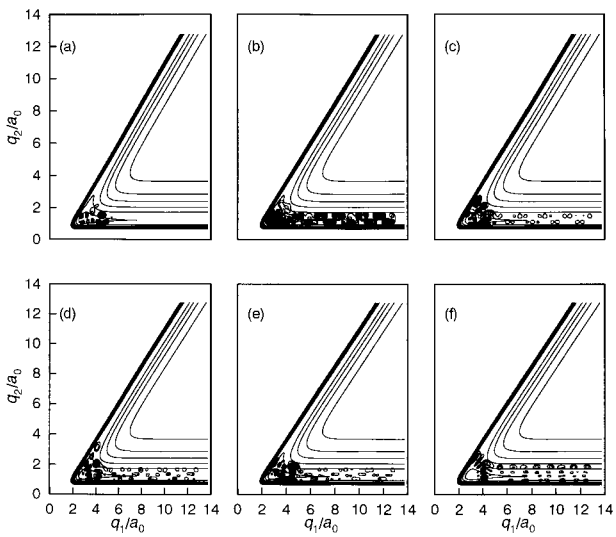

Fig. 4 Representative plots of $|\Psi|^2$ for different eigenfunctions of collinear HeH_2^+ that are difficult to assign—superimposed on the potential energy contours for the system: (a) 0.370, (b) 0.538, (c) 0.623, (d) 0.765, (e) 0.861 and (f) 0.974 eV.

Marston[22] had characterized some of the POs for collinear HeH_2^+ as belonging to *R*, *M* or *W* types, from a topological point of view. He computed the semiclassical eigenfunctions corresponding to these POs and showed that their time evolution and the resulting power spectra could account for many of the resonances. But there still remained a number of POs to be identified and their stability examined. Therefore we have undertaken a detailed investigation of the POs and their stabilities for collinear HeH_2^+ and its isotopic variants $HeHD^+$ and $HeDH^+$.

Preliminary investigations revealed that many of the POs have a complicated structure and are possibly unstable. The standard turning point algorithm and related ones[23] could locate the simple POs corresponding to either local or hyperspherical modes, but failed in locating the more complicated ones. Therefore, we had to use the Periodic Orbit Multiple Shooting (POMULT) algorithm[24] for locating the POs and studying their characteristics. In this approach, instead of trying to close the initial and final points of a single trajectory, several trajectories are integrated simultaneously by imposing the continuation conditions, while require the final point of one trajectory to coincide with the initial point of the next trajectory. To locate the principal families of POs (those that emerge from an equilibrium point of the potential) and their bifurcations we have constructed continuation/bifurcation (C/B) diagrams for a range of total energy values.[25]

We show in this paper that there are several period doubling bifurcations and families of POs for collinear (He, H_2^+) and (He, DH^+) and that the large number of resonances observed in the quantum calculations could be related to contributions from different members of the different families of periodic orbits, interspersed over the entire energy range of investigations. For collinear (He, HD^+) collisions, the principal families show an early transition to instability and remain unstable for the energy range studied. This explains the more chaotic structure of the phase space for this species.[16] For collinear (He, DH^+), the C/B diagram shows multiple changes in the stability of the principal families. Some simple bifurcating POs resemble a "horse-shoe" and are distinctly different from the hyperspherical ones.

After a short description of the numerical methods used in Section 2 the results of our investigations are presented and discussed in Section 3. A summary of our findings is given in Section 4.

2 Methodology

The PES used in the present calculations has been described elsewhere.[7] Taking the zero of energy to be that of the minimum of H_2^+, well separated from He, the minimum of the PES (−0.310 832 eV) for HeH_2^+ occurs at $q_1 = 3.068\,593\ a_0$ and $q_2 = 1.254\,757\ a_0$, where

$$q_1 = r_1 + \beta r_2 \sin\theta$$

and

$$q_2 = \beta r_2 \cos\theta$$

with r_1 the A–B distance and r_2 the B–C distance for a collinear arrangement of an atom A and a diatom BC. In the present study A = He and B and C are either H or D, depending upon the system under investigation. The terms β and θ are defined as

$$\beta = \sqrt{\frac{m_C(m_A + m_B)}{m_A(m_B + m_C)}}$$

and

$$\theta = \sin^{-1}\left[\frac{m_A m_C}{(m_A + m_B)(m_B + m_C)}\right]^{1/2}$$

The values used for the masses of the atoms in the calculations are: $m_H = 1.007\,97$ u, $m_D = 2.015\,94$ u and $m_{He} = 4.003$ u.

The exit channel, $HeH^+ + H$, is 0.7586 eV above the entrance channel. We hasten to add that the minima in the PES for collinear $HeHD^+$ and $HeDH^+$ occur at some other (q_1, q_2) values and that β and θ have slightly different values from that of HeH_2^+.[21]

Classical periodic orbits are located by multiple shooting algorithms and by damped and quasi-Newton iterative methods.[24] For a system with two degrees of freedom, there are two families of periodic orbits that emanate from the minimum of the potential. These families are called the principals and they correspond to the two normal vibrational modes. By following the evolution of the principal families with total energy, one can locate new families of POs, which bifurcate from the parent ones; they start either with the same periods as the original POs or with their multiples. New POs may also appear *via* saddle–node bifurcations. These bifurcations appear suddenly at particular excitation energies as pairs of periodic orbits with one of them being stable and the other being unstable.

A periodic orbit is stable when trajectories started close to it stay in its vicinity for all times. On the other hand, a PO is unstable when trajectories that are launched close to it depart exponentially, *i.e.*, the "distance" between the two trajectories in phase space grows exponentially with time. Whether a periodic orbit is stable or unstable is determined by the eigenvalues of the monodromy matrix, which is calculated by integrating the variational equations (*i.e.* the linearized difference equations of the two neighboring trajectories) together with the Hamilton equations.[25] When the eigenvalues lie on the unit complex circle, the POs are stable. When one or more pairs of the eigenvalues fall outside the unit circle, the PO is unstable.

3 Results and discussion

3.1 HeH_2^+

As per the existence theorem of Weinstein,[26] close to the equilibrium point there would be at least two periodic orbits with periods close to that of the linearized system for collinear HeH_2^+ and its isotopic variants. Therefore, we start our search for periodic orbits from the bottom of the potential well by locating the two principal families. One of them has a starting period (T) of 2.91 t.u. (1 t.u. = $0.538\,725 \times 10^{-14}$ s), denoted by **H** (for high frequency), and the other has a period of 7.22 t.u., labeled with **L** (for low frequency). The variation of T with E was investigated for each family and the results are shown in Fig. 5(a). In the process, the stability of the periodic orbit was examined and bifurcations were identified.

Three saddle–node bifurcation families (**SN1**, **SN2**, **SN3**) were also found at $E = 0.591\,15$ eV, $E = 0.756\,55$ eV and $E = 0.861\,92$ eV respectively. A projection of the C/B diagram in the (E, q_1) plane is shown in Fig. 5(b). Representative plots of POs from different families are depicted in Fig. 6. We show two members of each family, one at low energy and another usually at the highest available energy to show the evolution in their morphology. The initial conditions for these POs are listed in Table 3.

The **H** family starts at the minimum of the well in the PES, with stable POs that retain their stability up to $E = -0.19$ eV and $T = 3.08$ t.u. Above this energy, **H** undergoes a period doubling (PD) bifurcation giving rise to the initially stable **H1A** family. The stability of the **H** family is regained around $E = 0.17$ eV (3.8), wherein another PD bifurcation takes place. The number in parentheses refers to T in t.u. at that energy. The **H** family remains stable until the energy reaches roughly 2.4415 eV (9.15). The lowest energy PO of the **H1A** family is

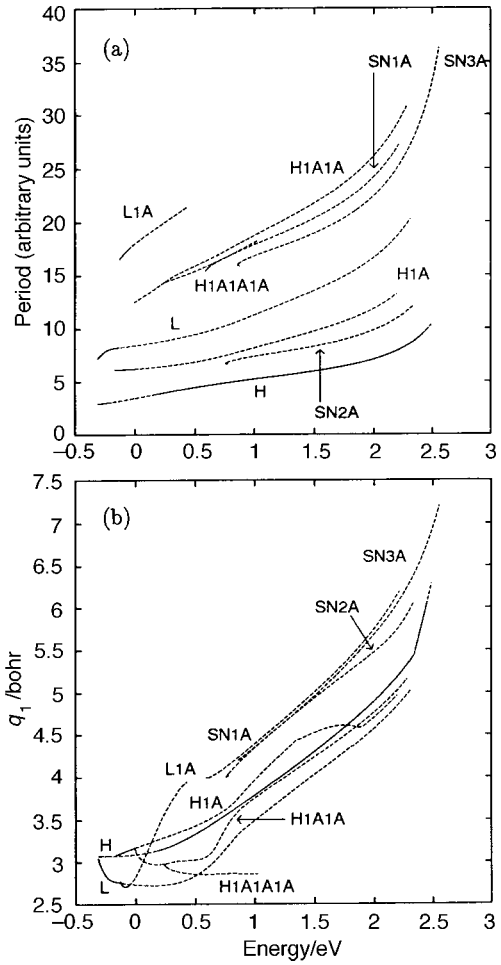

Fig. 5 Continuation/bifurcation diagram for collinear HeH_2^+. (a) The variation of the period (T) of the periodic orbits in different families with the total energy E. (b) The initial value of q_1 *versus* the total energy E for different families of POs. The solid lines represent stable periodic orbits and the dotted lines unstable periodic orbits.

located at $E = -0.177\,07$ eV (6.1747). This family is stable until E becomes -0.008 eV (6.235). The PD bifurcation at that energy gives birth to the **H1A1A** family, rendering **H1A** unstable.

The **H1A1A** family starts with a period of roughly 12.474 t.u. around $-0.007\,67$ eV. It is stable up to 0.02 eV (12.65), around which a PD bifurcation takes place. Another PD bifurcation restores the stability at 0.215 eV (14.1). No attempt was made to locate the two emanating families due to the higher expected period. Around 0.241 eV (14.32) a "simple" bifurcation occurs and a pair of families is born. The stable branch has been located and is denoted by **H1A1A1A**. The **H1A1A** family "ends", according to presently available data, as unstable at 2.28 eV (30.8), seemingly heading towards another simple bifurcation.

The first located PO of the **H1A1A1A** family is at 0.242 eV (14.324). It is unstable up to 0.253 eV (14.37), where a PD bifurcation takes place and it ends up highly unstable at 0.89 eV (17.414).

L is the other principal family emanating from the equilibrium point. The first orbit located of the **L** family is at -0.3098 eV, with a period of 7.22 t.u. This family comes very close to a PD bifurcation (the two eigenvalues of the monodromy matrix are almost equal to -1) roughly at the energy of -0.3072 eV when $T = 7.25$ t.u., but remains stable. Close to $E = -0.129$ eV (8.27) a PD bifurcation occurs, changing the stability of the family and giving birth to the **L1A** family. The instability of the **L** family grows steadily, at least until 2.3 eV is reached.

The **L1A** family has the first located member at $E = -0.1282$ eV (16.55). It loses its stability *via* a PD bifurcation around -0.103 eV (16.9). Stability is restored through another PD bifurcation at -0.087 eV (17.12). Close to $E = -0.060$ eV (17.42) a simple bifurcation generates a pair of families; they were not located. The **L1A** family "ends" as highly unstable at 0.428 eV (21.37).

At $E = 0.591\,16$ eV a saddle–node bifurcation gives rise to the **SN1** families. Their initial period is at 15.387 t.u. The stable branch (**SN1A**) is destabilized *via* a simple bifurcation very early. Our data for it stop at 2.215 eV (27.2). The unstable one is very short.

The pair of **SN2** families is generated at $E = 0.756\,55$ eV with a period of 6.7339 t.u. The stable branch (**SN2A**) undergoes a PD bifurcation around 0.762 eV (6.8) and "ends" as unstable at 2.34 eV (12.12).

A third pair of saddle–node families **SN3** has been located at 0.8619 eV (15.97). The stable branch of the two (**SN3A**) loses its stability roughly at 0.8645 eV (16.04). It "ends" as highly unstable at 2.557 eV (36.321). As with the other saddle–node families, it was very difficult to continue the unstable branch for an extended energy range.

Looking at Fig. 6 we note that the **SN2** and **SN3** saddle–node POs are those which penetrate into the exit channel of the potential, contrary to **L** type POs which penetrate into the entrance channel.

Table 3 Initial conditions for representative periodic orbits of collinear HeH_2^+; distances are in a_0, masses in u, energy in eV and time in units of 5.38725 fs

Family	Energy	Period	q_1	q_2	p_1	p_2
H	0.26131	3.995	3.169733	1.9552364	0.17837509	−0.31611063
H	2.48212	10.215	6.2414811	3.9982721	0.55558333	−0.61881186
H1A	−0.10538	6.1874	3.1147197	1.0690562	−0.26477449	0.27816479
H1A	2.15121	12.8524	4.8998705	3.4119527	−1.1592584	1.0427609
H1A1A	0.02733	12.714	3.0590249	1.0216088	−0.32084893	0.35052733
H1A1A	2.26167	30.394	5.1239475	3.7807941	1.3586777	−0.94825122
H1A1A1A	0.25006	14.354	2.9505148	1.2848051	−0.20538347	1.1960344
H1A1A1A	1.00765	18.114	2.8575151	1.7657996	0.90609617	1.0874973
L	−0.15011	8.24	2.7573698	1.3182378	−0.31105752	0.26485164
L	2.28376	19.825	4.97958	3.6302386	1.3022264	−1.1316926
L1A	−0.12731	16.57	2.7660476	1.2932308	−0.35167411	0.38854866
L1A	0.4172	21.29	3.9298047	1.3975187	0.52569251	−1.040838
SN1	0.59445	15.48693	3.9928318	1.5034585	−0.12185323	1.2273031
SN1	2.20567	27.03694	6.1719682	2.964	−0.08893741	0.71872422
SN2	0.769	6.8339	4.0252328	2.3763803	0.38715819	0.02602432
SN2	2.32655	11.9939	6.030285	3.7256859	−0.67375014	0.00727356
SN3	0.86246	16.0007	4.2013443	2.402138	0.083503626	0.013920686
SN3	2.55215	36.0007	7.1797603	4.1541895	−0.1816258	−0.058834976

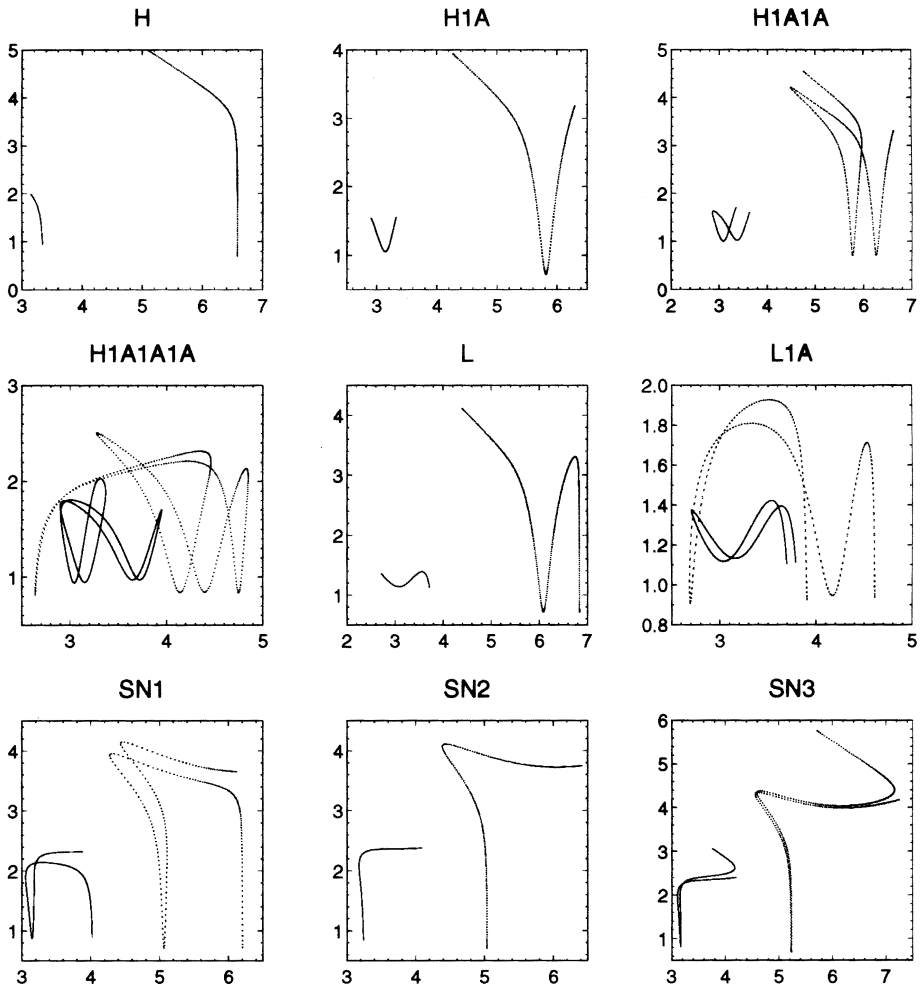

Fig. 6 Plots of representative periodic orbits in the coordinate plane (q_1, q_2) for collinear HeH_2^+. Two POs of each family are shown, one at low energy and another at the highest available energy.

3.2 $HeHD^+$

For collinear $HeHD^+$ the minimum of the PES occurs at $q_1 = 3.409\,684\,9\ a_0$ and $q_2 = 1.278\,220\,1\ a_0$. Two families of periodic orbits were found to emanate from it; one of them has a starting period of 3.32 t.u., and is denoted by **H** as before. The other has a larger period (8.3 t.u.) and is labeled **L**. A C/B diagram for the system is shown in the form of *T versus E* plot for different families of POs in Fig. 7(a). A q_1 *vs.* *E* plot is presented in Fig. 7(b). Representative plots of periodic orbits from different families are depicted in Fig. 8 and their initial conditions are listed in Table 4.

The lowest energy periodic orbit found for the **H** family has a period of 3.325 t.u. at $E = -0.306\,73$ eV. The family is stable up to -0.192 eV (3.495), around which a PD bifurcation occurs and the **H1A** family is born. The **H** family continues as slightly unstable until 2.1 eV (8.32).

The **H1A** family starts around $-0.194\,24$ eV (6.984). Close to -0.0262 eV (7.02) a PD bifurcation generates the **H1A1A** family, which inherits the stability over a limited energy range. The **H1A** family ends, according to available data, at 2.178 13 eV (14.7313) as unstable.

The **H1A1A** family has the first located orbit at -0.025 eV (14.05). It loses its stability quickly; around -0.005 eV (14.17) a PD bifurcation takes place. At 0.448 95 eV (17.0), another PD bifurcation restores the stability. Around 1.212 75 eV (22.09), a PD bifurcation renders the family unstable. It ends at 2.191 15 eV (32.29).

The first PO of the **L** family is located at $-0.308\,23$ eV, with a period of 8.3 t.u. Its stability is lost at -0.15 eV (9.37), around which a PD bifurcation generates the **L1A** family. The instability of **L** rapidly increases at least until 2.0 eV (18.7) is reached.

L1A is slightly more interesting: it was found to start as stable at -0.1494 eV (18.76). The stability alternates through two PD bifurcations, one at -0.124 eV (19.18) and another around -0.11 eV (19.4). A "simple" bifurcation occurs at roughly -0.083 eV (19.74), giving rise to **L1A1A** and destabilizing **L1A**. The family ends as highly unstable at 0.437 58 eV (24.31).

The **L1A1A** family starts almost at $-0.080\,95$ eV (19.76). A PD bifurcation at -0.073 eV (19.79) destroys its stability. Available data end at 0.291 eV (21.68). In the continuation diagram, Fig. 7(b), **L1A1A** follows almost exactly the **L1A** family; they are different though.

3.3 $HeDH^+$

For the isotopic variant $HeDH^+$ the potential energy minimum occurs at $q_1 = 2.727\,501\,5\ a_0$ and $q_2 = 1.278\,220\,0\ a_0$. Two families of periodic orbits are found to emanate from it; the **H** has a starting period of 3.348 t.u., whereas the **L** has a period of 8.2 t.u. A plot of q_1 *vs.* *E* of the initial conditions for these families and their bifurcations is presented in Fig. 9. Fig. 10 is a graph of the period of each orbit as a function of its energy. Representative plots of periodic orbits from the different families are depicted in Fig. 11. Their initial conditions are given in Table 5.

The **H** family starts from the potential minimum. The first located orbit has a period of 3.348 t.u. at -0.3098 eV. The family loses and gains stability through two PD bifurcations; one around -0.158 eV (3.636), generating the **H1A** family,

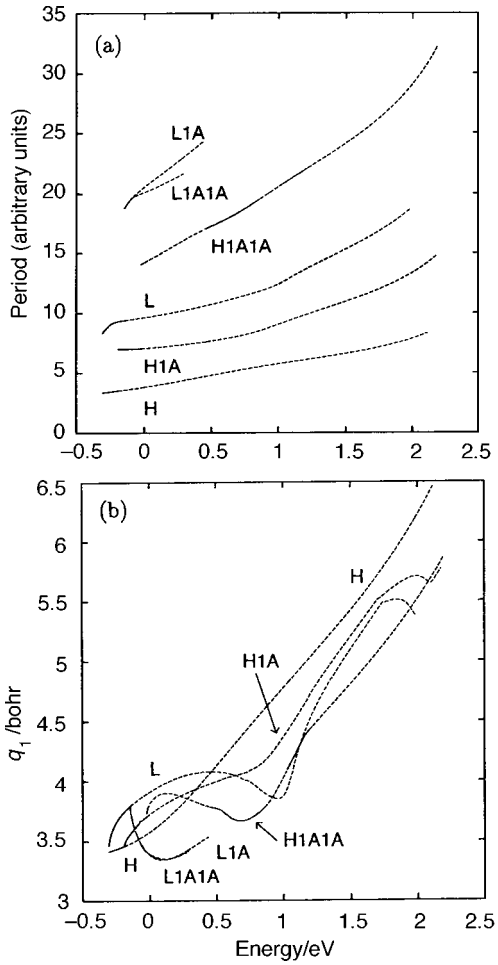

Fig. 7 Continuation/bifurcation diagram for collinear $HeHD^+$. (a) The variation of T with E for different families of POs. (b) The initial value of q_1 *versus* the total energy E for different families of POs. The solid lines represent stable periodic orbits and the dotted lines represent unstable periodic orbits.

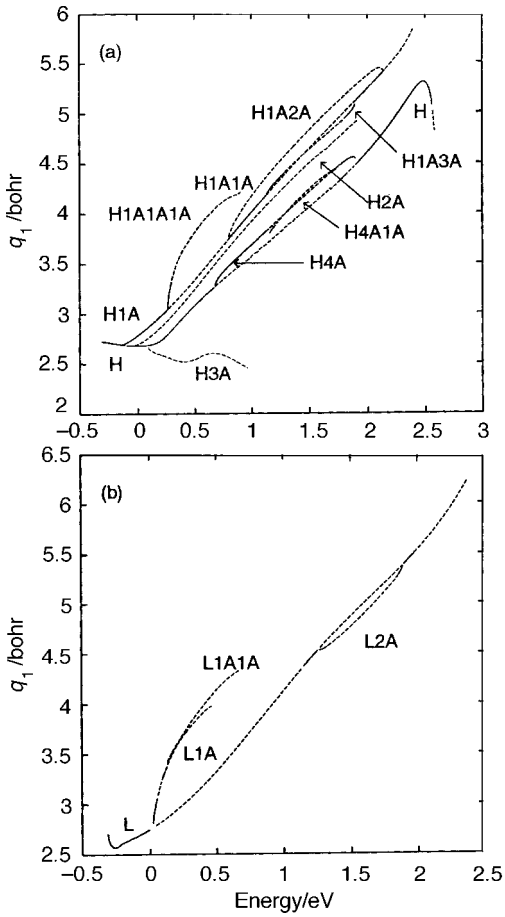

Fig. 9 Continuation/bifurcation diagram for collinear $HeDH^+$. Plotted is the initial value of q_1 *versus* the total energy E. (a) the **H** family and bifurcations from it and (b) the **L** family and its bifurcations. The solid lines represent stable periodic orbits and the dotted lines unstable periodic orbits.

and the other at −0.08 eV (3.816), giving birth to the family labeled **H2A**. Around 0.087 eV (4.346) two conjugate eigenvalues of th monodromy matrix acquire the value $e^{\pm i2\pi/3}$, producing a 1 : 3 resonance and the **H3A** family.

The **H** family is stable until its energy becomes 0.67 eV and the period is 5.85 t.u. A "simple" bifurcation there generates the **H4A** family. The stability is restored at 1.895 eV (8.18) through another bifurcation. Around this point, the **H4A** family again joins the **H** family. At roughly 2.148 eV (15.125) a

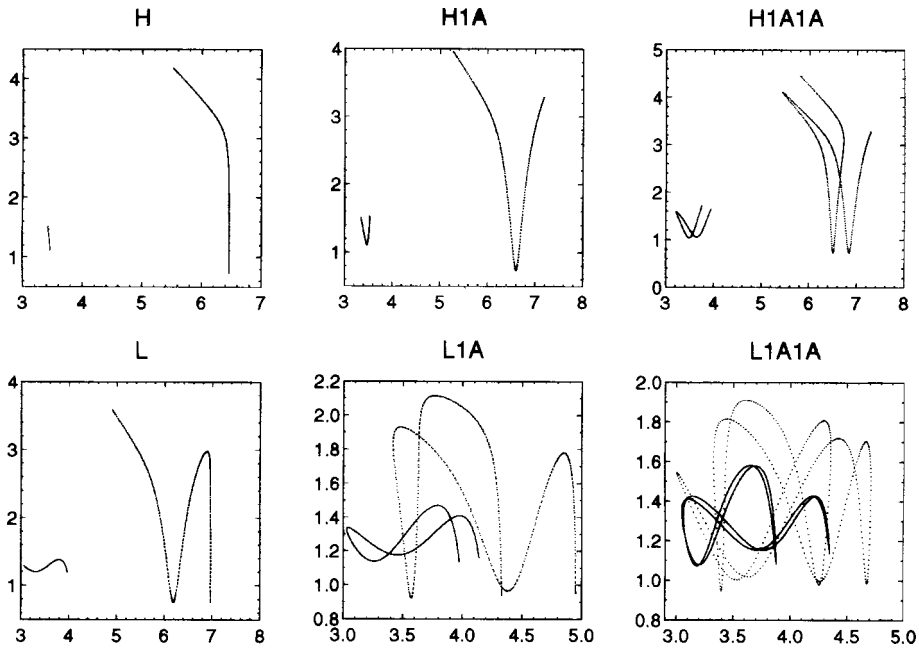

Fig. 8 Plots of representative periodic orbits in the coordinate plane (q_1, q_2) for collinear $HeHD^+$. Two POs of each family are shown, one at low energy and another at the highest available energy.

Table 4 Initial conditions for representative periodic orbits of collinear $HeHD^+$; the units are listed in Table 3

Family	Energy	Period	q_1	q_2	p_1	p_2
H	−0.18907	3.5	3.4591727	1.1765241	0.032706073	−0.52928436
H	2.10984	8.3	6.4512147	2.4374391	−0.034938435	1.4993002
H1A	−0.17824	6.97995	3.5101456	1.2772609	−0.0707593	−0.6603505
H1A	2.17272	14.6813	5.7634009	3.4213711	−1.190251	1.3661556
H1A1A	−0.0007	14.2	3.8143053	1.3050231	−0.33659634	−0.87733407
H1A1A	2.18920	32.25	5.8556467	3.5893622	1.1633728	−1.4878306
L	−0.20099	9.275	3.734687	1.3671398	−0.41412862	−0.12341713
L	1.98145	18.695	5.3834065	3.056116	−1.1356015	1.3282091
L1A	−0.14269	18.88	3.730791	1.4558494	−0.4365974	−0.17746542
L1A	0.43758	24.31	3.5322334	1.0864824	−0.22488994	1.3970472
L1A1A	−0.08095	19.76	3.5173822	1.5175962	−0.46089912	−0.41839418
L1A1A	0.29108	21.68	3.414646	1.1484151	−0.06679529	−1.3591841

PD bifurcation destroys the stability. The family ends, according to presently available data, at 2.583 eV (14.331) as stable.

The **H1A** family starts close to −0.149 73 eV (7.29). It inherits the stability of the **H** family. It then loses it through a PD bifurcation at 0.26 eV (7.79), generating the **H1A1A** family. It becomes stable again through another PD bifurcation at 0.795 eV (9.15), generating the family labeled **H1A2A**.

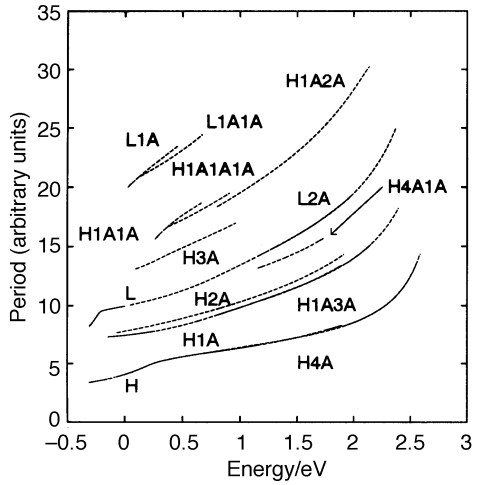

Fig. 10 The variation of T with E for different families of POs for collinear $HeDH^+$. The solid lines represent stable periodic orbits and the dotted lines unstable periodic orbits.

Around 1.125 eV (10.245) the **H1A** family undergoes a bifurcation, generating **H1A3A** with which it recombines at 1.9 eV (13.37) through another bifurcation. At 2.1477 eV (15.125), in a PD bifurcation, **H1A2A** merges with **H1A**. The **H1A** family "ends" as unstable at 2.39 eV, 18.185 t.u.

The **H2A** family starts around −0.070 43 eV (7.65). It is highly unstable throughout until it "ends" at 1.91 eV (14.31). The **H3A** family was found to start at 0.0926 eV (13.08). It is highly unstable until it "ends" at 0.971 eV (17). The **H4A** family starts roughly at 0.6783 eV (5.86). It is stable up to 1.145 eV (6.56), where a PD bifurcation generates **H4A1A**. In another PD bifurcation, at 1.73 eV (7.82), it recombines with **H4A1A**. The **H4A** family ends as stable at 1.896 eV (8.277), when through a bifurcation it merges with **H**.

The **H1A1A** family starts around 0.2605 eV (15.6). It loses its stability at 0.295 eV (15.97) and regains it at 0.35 eV (16.49) through PD bifurcation. Close to 0.365 eV (16.62), a bifurcation results in the **H1A1A1A** family. The **H1A1A** family ends as highly unstable at 0.656 93 eV (18.6).

The **H1A2A** family starts around 0.7976 eV (18.33). It is highly unstable through its "lifetime". It merges with **H1A** through a PD bifurcation at 2.1477 eV (30.25).

Table 5 Initial conditions for representative periodic orbits of collinear $HeDH^+$; the units are listed in Table 3

Family	Energy	Period	q_1	q_2	p_1	p_2
H	−0.20995	3.526	2.7053395	1.118915	−0.00092153	−0.034586715
H	2.46618	11.931	5.2969186	3.8259113	−0.46470513	0.62496345
H1A	−0.14266	7.295	2.6893398	1.118363	0.09680772	−0.46735715
H1A	2.00528	14.025	5.246813	2.9335439	−0.12999278	−0.48871107
H2A	−0.05982	7.67	2.6813498	1.6123351	0.20261948	0.38382493
H2A	1.90718	14.29	4.9164961	2.9082905	0.27405412	−0.3849385
H3A	0.10052	13.11	2.6496185	1.0214163	0.0977416	0.58438506
H3A	0.95471	16.92	2.4604799	1.474194	1.2743121	1.5053238
H4A	0.68361	5.867	3.3055731	1.6876094	−0.14458188	1.3790343
H4A	1.89419	8.275	4.5472003	3.1653343	−0.45411267	0.30910669
H1A1A	0.26212	15.62	3.0788544	1.0732026	0.52130509	−0.98735254
H1A1A	0.65196	18.6	4.0133766	1.3279419	0.2302487	1.5634009
H1A2A	0.80619	18.38	3.8014993	1.2774635	0.37866144	1.7506787
H1A2A	2.13086	30.18	5.4219962	1.5104501	−0.19870247	−2.5788208
H1A3A	1.13629	10.28	4.207528	1.8424713	0.25143154	1.3789079
H1A3A	1.88814	13.34	5.0678261	2.8887089	−0.16668871	−0.22652227
H4A1A	1.72302	15.6	4.4281135	2.9678135	−0.30976339	0.26336434
H4A1A	1.16246	13.17	3.8184833	1.8990842	0.26702839	1.4274146
H1A1A1A	0.38699	16.72	3.6215516	0.9851035	0.31465026	0.65439347
H1A1A1A	0.89687	19.44	4.2072508	1.9144245	−0.20927038	−0.86884635
L	−0.05412	9.845	2.7077265	1.1792751	0.67642724	−0.55231624
L	2.36744	24.945	6.2059083	1.2482586	−0.0064722	2.8570706
L1A	0.02803	20.05	2.8732798	1.1581154	0.72084206	−0.66535868
L1A	0.45758	23.51	3.9741865	1.243436	0.38489452	1.333635
L2A	1.26898	14.73	4.5286066	2.2525702	0.32322068	0.53171956
L2A	1.88301	18.48	5.3463451	2.3767204	0.06218402	−1.2892722
L1A1A	0.13074	20.94	3.4239548	1.0406756	0.55512386	−0.16135752
L1A1A	0.65956	24.38	4.3223818	1.4991339	−0.0100025	−1.3654216

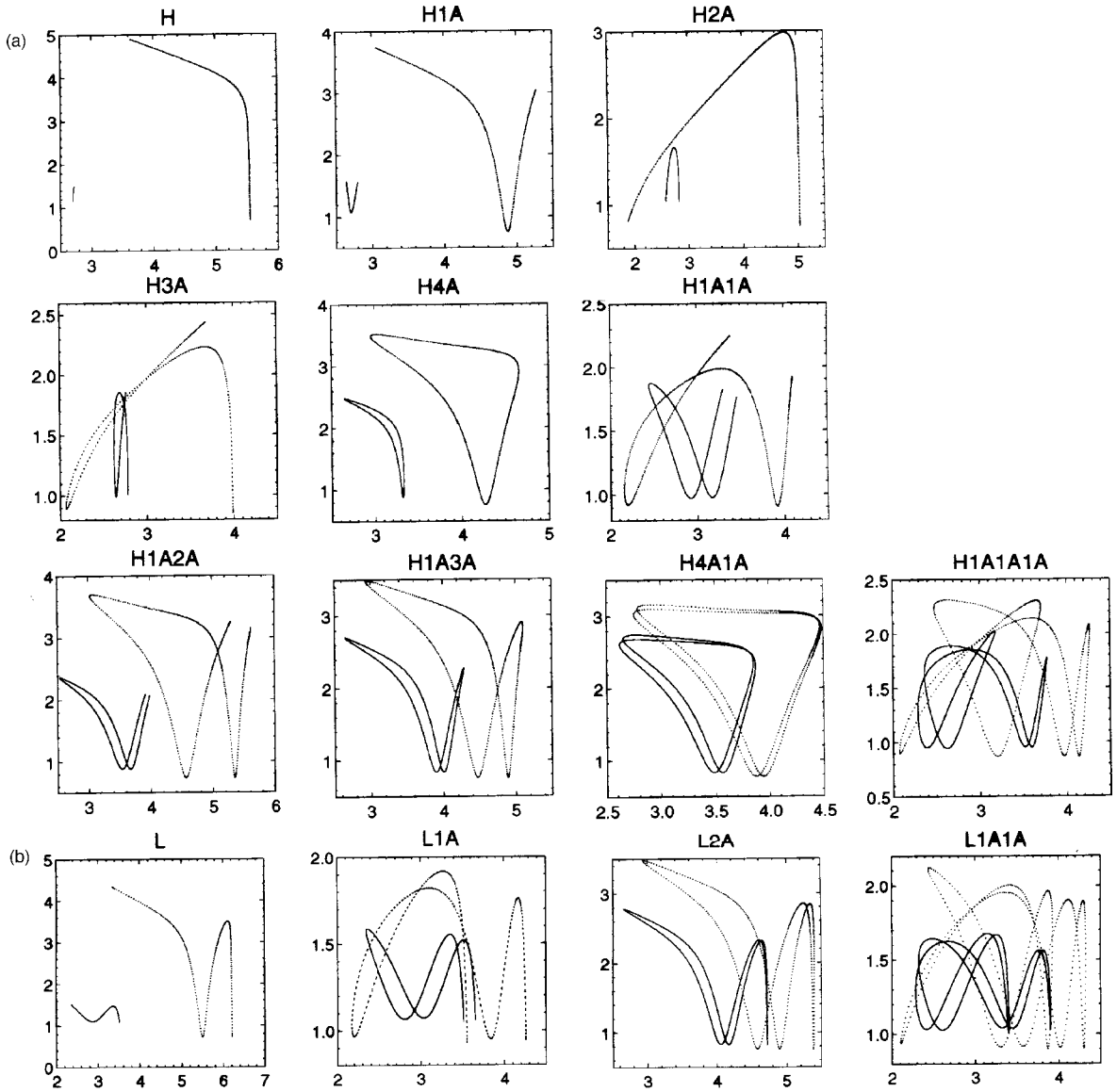

Fig. 11 Plots of representative periodic orbits in the coordinate plane (q_1, q_2) for collinear $HeDH^+$. Two POs of each family are shown, one at low energy and another at the highest available energy for (a) the **H** related families and (b) the **L** related families.

The **H1A3A** family starts at 1.13 eV (10.26). It alternates in stability through two PD bifurcations, one around 1.28 eV (10.75) and another at 1.822 eV (13.01). It becomes stable at 1.9 eV (13.37), when it recombines with **H1A** through a simple bifurcation.

The **H4A1A** family starts roughly at 1.154 eV (13.14) as stable. The stability toggles through two PD bifurcations, one at 1.21 eV (13.34) and another at 1.695 eV (15.44). The family ends at 1.73 eV (15.63) by merging with **H4A** in a PD bifurcation.

The **H1A1A1A** family has the first located member at 0.377 94 eV (16.68). It is highly unstable at least up to 0.9035 eV (19.48). In the continuation diagram, Fig. 9(a), it follows **H1A1A** closely.

The **L** family starts in the potential well. The first orbit was found at −0.3105 eV (8.2). It comes very close to a PD bifurcation at −0.30 eV (8.325) but it is not destabilized. Around 0.023 eV (10.0), a PD bifurcation destabilizes **L** and gives birth to **L1A**. The **L** family is unstable until 1.14 eV (14.1), around which it undergoes a PD bifurcation. At roughly 1.2627 eV (14.7) a simple bifurcation generates **L2A**. The stability is restored at 1.8926 eV (18.5) through another bifurcation; there **L2A** recombines with **L**. At 2.0 eV (19.5), a PD bifurcation destroys the stability of **L**. It "ends" as unstable at 2.37 eV (25).

The **L1A** family starts from 0.023 eV (20) as stable. It undergoes three PD bifurcations: around 0.055 (20.33), 0.09 (20.64) and 0.125 eV (20.92). It "ends" as highly unstable at 0.65 eV (24.3).

The **L2A** family starts around 1.2627 eV (14.7) and it is stable up to 1.325 eV (15), where a PD bifurcation takes place. Stability is restored at 1.852 eV (18.25) through another PD bifurcation. The **L2A** family merges with **L** *via* a simple bifurcation.

It is clear from the C/B diagrams in Figs. 5, 7, 9 and 10 that the two principal families lead to several other families and that the route to chaos in the system is (at least partly) through period doubling. In the case of collinear HeH_2^+, the **H** family is stable over most of the energy range under investigation. As a matter of fact, it is the only family that is stable over that range of E. The same family becomes unstable for $HeHD^+$ under similar conditions. But it remains stable over most of the range of E for $HeDH^+$, although there is substantial overlap with the unstable **H4A** family in the (E, T) space, POs of the **H** family are hyperspherical (called the R type by Marston[22]) for all the three systems (HeH_2^+, $HeHD^+$ and $HeDH^+$). Members of **H1A** have a "V" shape and those of **H1A1A** are of "W" type (as named by Marston). **H1A1A1A** is not present in $HeHD^+$, but is similar for HeH_2^+ and $HeDH^+$. Members of the **L** and **L1A** families are similar in

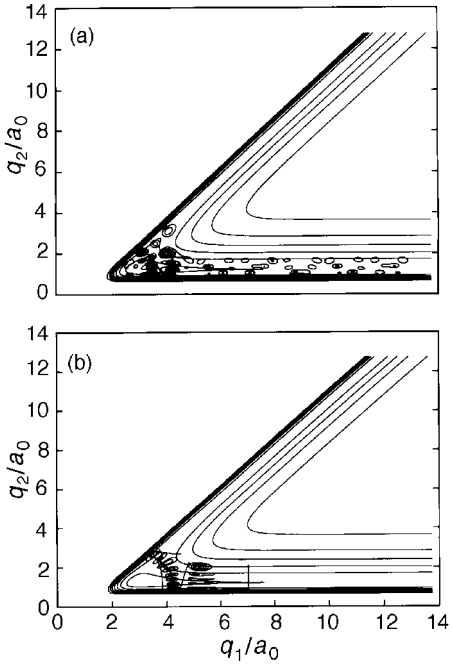

Fig. 12 Plots of $|\Psi|^2$ for different eigenfunctions of collinear HeH_2^+, superimposed on the potential energy contours for the system, along with the POs at that energy: (a) 0.7653 and (b) 1.1339 eV.

shape for HeH_2^+ and $HeHD^+$. We have been able to locate the **SN1**, **SN2** and **SN3** families for HeH_2^+. These are periodic orbits which penetrate into the exit channel. Members of the **SN1** family correspond to the "M" type POs identified by Marston. $HeDH^+$ is unique in that its POs show far too many PD bifurcations and its $P_v^R(E)$ plots show the largest numbers of oscillations among the three systems (see Fig. 7 of ref. 14). "Boomerang" type (**H1A** and **H4A1A**) and closed "W" type (**H1A3A**) POs are seen only for $HeDH^+$. Since none of the families of POs is stable for $HeHD^+$, there is much less bifurcation in it.

Eigenfunctions of HeH_2^+ that can be characterized in terms of quantum numbers corresponding to hyperspherical coordinates are nearly superimposable on POs of the **H** family at the corresponding energies, as illustrated in Fig. 3. However, the eigenvalue spectrum for collinear HeH_2^+ is still far from being regular because of the contributions from unstable POs of other families. It becomes clear from the contour plots of $|\Psi|^2$ at $E = 0.7653$ eV shown in Fig. 12(a), for example, that the structures can be accounted for only partly by the superposed PO of **H1A** family at that energy. Contour plots of $|\Psi|^2$ at $E = 1.1339$ eV in Fig. 12(b) suggest that the PO at that energy should have at least partly hyperspherical character. We have located three POs at that energy: one from the **H1A** family, one from the **SN2** family and one that is indicative of the reactant vibrational mode. We have plotted them all in Fig. 12(b). It is clear that the shape of the eigenfunction is not fully accounted for. It is also clear that it would be practically impossible to assign all the peaks in the spectrum in Fig. 1.

4 Summary and conclusions

We have carried out a systematic investigation of the different families of POs and constructed their C/B diagrams over a wide range of energy values for collinear HeH_2^+, $HeHD^+$ and $HeDH^+$ systems. Some of the POs are of local mode type and some are of the hyperspherical variety. There are more complicated ones too. Except for the ones near the equilibrium point and the **H** family over a wide range of E for HeH_2^+ and $HeDH^+$, most of the other POs are unstable and often lead to period doubling bifurcation, thus suggesting the route to classical chaos in the system.

While some of the peaks in the spectrum for collinear HeH_2^+ for example could be assigned to hyperspherical modes of increasing excitation with increase in energy, most of the other peaks can not be accounted for readily. They seem to arise from a superposition of contributions from POs of different families at a given energy. The C/B diagram for collinear HeH_2^+ reveals a number of bifurcations and families of POs and that for $HeDH^+$ reveals an even larger number of period doubling bifurcations and families of POs. Therefore, plots of $P_v^R(E)$ for HeH_2^+ and $HeDH^+$ are highly oscillatory. There are relatively less bifurcations and families of POs for $HeHD^+$ and the $P_v^R(E)$ plots of the system contain the least number of oscillations.

Thus it is gratifying to see that a systematic analysis of the stability of POs provides an insight into the origin of classical chaos and also into the nature and cause of irregularity in the eigenvalue spectrum and transition state resonances in collinear HeH_2^+ and its isotopic variants.

Acknowledgements

This study was supported in part by a grant from the Department of Science and Technology, New Delhi, India. We are grateful to Drs. R. Ramaswamy and K. Srihari for their comments on an earlier version of the manuscript.

References

1 D. J. Kouri and M. Baer, *Chem. Phys. Lett.*, 1974, **24**, 37.
2 J. T. Adams, *Chem. Phys. Lett.*, 1975, **33**, 275.
3 P. J. Kuntz, *Chem. Phys. Lett.*, 1972, **16**, 581.
4 F. M. Chapman Jr. and E. F. Hayes, *J. Chem. Phys.*, 1975, **62**, 4400; 1976, **65**, 1032.
5 T. Joseph and N. Sathyamurthy, *J. Indian Chem. Soc.*, 1985, **62**, 874.
6 D. R. McLaughlin and D. L. Thompson, *J. Chem. Phys.*, 1979, **70**, 2748.
7 T. Joseph and N. Sathyamurthy, *J. Chem. Phys.*, 1987, **86**, 704.
8 N. Sathyamurthy, M. Baer and T. Joseph, *Chem. Phys.*, 1987, **114**, 73.
9 J. Manz, *Comments At. Mol. Phys.*, 1985, **17**, 91.
10 K. Sakimoto and K. Onda, *Chem. Phys. Lett.*, 1994, **226**, 227.
11 N. Balakrishnan and N. Sathyamurthy, *Chem. Phys. Lett.*, 1993, **201**, 294; 1995, **240**, 119.
12 S. Mahapatra and N. Sathyamurthy, *J. Chem. Phys.*, 1995, **102**, 6057.
13 S. Mahapatra, R. Ramaswamy and N. Sathyamurthy, *J. Chem. Phys.*, 1996, **104**, 3989.
14 V. Balasubramanian, B. K. Mishra, A. Bahel, S. Kumar and N. Sathyamurthy, *J. Chem. Phys.*, 1991, **95**, 4160; A. Rahaman and N. Sathyamurthy, *J. Chem. Phys.*, 1994, **98**, 12481.
15 S. Mahapatra and N. Sathyamurthy, *J. Chem. Phys.*, 1996, **105**, 10934.
16 S. Mahapatra, N. Sathyamurthy and R. Ramaswamy, *Pramana–J. Phys.*, 1997, **48**, 411.
17 K. Sakimoto, *J. Chem. Soc., Faraday Trans.*, 1997, **93**, 791.
18 S. C. Farantos, H.-M. Keller, R. Schinke, K. Yamashita and K. Morokuma, *J. Chem. Phys.*, 1996, **104**, 10055.
19 C. Beck, H.-M. Keller, S. Yu. Grebenshchikov, R. Schinke, S. C. Farantos, K. Yamashita and K. Morokuma, *J. Chem. Phys.*, 1997, **107**, 9818.
20 S. C. Farantos, C. Beck and R. Schinke, *Theor. Chem. Acc.*, 1998, **100**, 147.
21 S. Glasstone, K. J. Laidler and H. Eyring, *The Theory of Rate Processes*, McGraw-Hill, New York, 1941, p. 101.
22 C. C. Marston, *J. Chem. Phys.*, 1995, **103**, 8456.
23 E. Pollak, in *Theory of Chemical Reaction Dynamics*, ed. M. Baer, CRC Press, Boca Raton, FL, 1985, vol. III, ch. 2.
24 S. C. Farantos, *Comput. Phys. Commun.*, 1998, **108**, 240.
25 S. C. Farantos, *Int. Rev. Phys. Chem.*, 1996, **15**, 345.
26 A. Weinstein, *Inv. Math.*, 1973, **20**, 47.

Paper 8/08368A